Neurotransmitter-Responsive Nanosensors for T2-Weighted Magnetic Resonance Imaging

Citation: Hsieh, Vivian et al. "Neurotransmitter-Responsive Nanosensors for T2-Weighted Magnetic Resonance Imaging." Journal of the American Chemical Society 141, 40 (September 2019): 15751–15754 © 2019 American Chemical Society

As Published: http://dx.doi.org/10.1021/jacs.9b08744

Publisher: American Chemical Society (ACS)

Persistent URL: https://hdl.handle.net/1721.1/125916

Version: Author's final manuscript: final author's manuscript post peer review, without publisher's formatting or copy editing

Neurotransmitter-responsive nanosensors for T_2-weighted magnetic resonance imaging

Vivian Hsieh,[†] Satoshi Okada,[†,‡] He Wei,[†] Isabel García-Álvarez,[†,§] Ali Barandov,[†] Santiago Recuenco Alvarado,[†] Robert Ohlendorf,[†] Jingxuan Fan,[†] Athena Ortega,[†] and Alan Jasanoff*[,†]

[†]Department of Biological Engineering, Brain and Cognitive Sciences, and Nuclear Science and Engineering, Massachusetts Institute of Technology, 77 Massachusetts Avenue, Cambridge, Massachusetts 02139, United States

[‡]Health Research Institute, National Institute of Advanced Industrial Science and Technology, 1-1-1 Higashi, Tsukuba, Ibaraki 305-8566, Japan

[§] Faculty of Experimental Sciences, Francisco de Vitoria University (UFV), Ctra. Pozuelo-Majadahonda Km 1.800, Pozuelo de Alarcon, 28223 Madrid, Spain

Supporting Information Placeholder

ABSTRACT: Neurotransmitter-sensitive contrast agents for magnetic resonance imaging (MRI) have recently been used for mapping signaling dynamics in live animal brains, but paramagnetic sensors for T_1-weighted MRI are usually effective only at micromolar concentrations that themselves perturb neurochemistry. Here we present an alternative molecular architecture for detecting neurotransmitters, using superparamagnetic iron oxide nanoparticles conjugated to tethered neurotransmitter analogs and engineered neurotransmitter binding proteins. Interactions between the nanoparticle conjugates result in clustering that is reversibly disrupted in the presence of neurotransmitter analytes, thus altering T_2-weighted MRI signals. We demonstrate this principle using tethered dopamine and serotonin analogs, together with proteins selected for their ability to competitively bind either the analogs or the neurotransmitters themselves. Corresponding sensors for dopamine and serotonin exhibit target-selective relaxivity changes of up to 20%, while also operating below endogenous neurotransmitter concentrations. Semisynthetic magnetic particle sensors thus represent a promising path for minimally perturbative studies of neurochemical analytes.

Recent years have seen substantial advances in technology for mapping neurochemical dynamics in the brain.[1-3] Magnetic resonance imaging (MRI) methods in particular offer an attractive combination of minimal invasiveness, ability to monitor large fields of view, and relatively high resolution for studies in animals.[4] A basis for efforts to directly image monoamine neurotransmitters by MRI has been a set of sensors derived from the heme domain of the bacterial cytochrome P450-BM3 (BM3h).[5] BM3h variants engineered for selective binding to dopamine and serotonin produce ligand-dependent changes in longitudinal relaxation time (T_1), allowing corresponding neurotransmitters to be detected in T_1-weighted MRI.[6] Although BM3h-based probes have been used to map monoamine dynamics *in vivo*,[7,8] they produce relatively weak effects in MRI, as reflected by the slope of T_1 *vs.* probe concentration (relaxivity, r_1). With relaxivity values of 1-2 $mM^{-1}s^{-1}$, these sensors must be applied at concentrations that substantially exceed physiological levels of neurotransmitter analytes in brain interstitium. This in turn perturbs endogenous neurotransmitter concentrations and limits sensitivity of detection.

MRI probes based on superparamagnetic iron oxide nanoparticles (SPIOs) could offer a solution to these problems.[9,10] SPIOs can be detected at subnanomolar particle concentrations by transverse relaxation time (T_2)-weighted MRI. Reversible aggregation of SPIOs affords a versatile and sensitive mechanism for molecular detection.[11] Recently, this mechanism was applied to detect dynamic calcium signaling events in the brain,[12] indicating its potential for *in vivo* applications to other analytes.

To adapt SPIOs for sensing neurotransmitters, we initially targeted dopamine. Figure 1a depicts a candidate dopamine responsive nanoparticle (DaReNa) probe consisting of two populations of modified SPIOs, one conjugated to a dopamine-binding protein, and the other attached to a tethered analog capable of competing with dopamine for protein binding. In the absence of dopamine, the two types of SPIOs should form clusters with altered T_2 relaxivity (r_2), compared with individual particles. In the presence of dopamine, interactions between particles should be disrupted by competition,

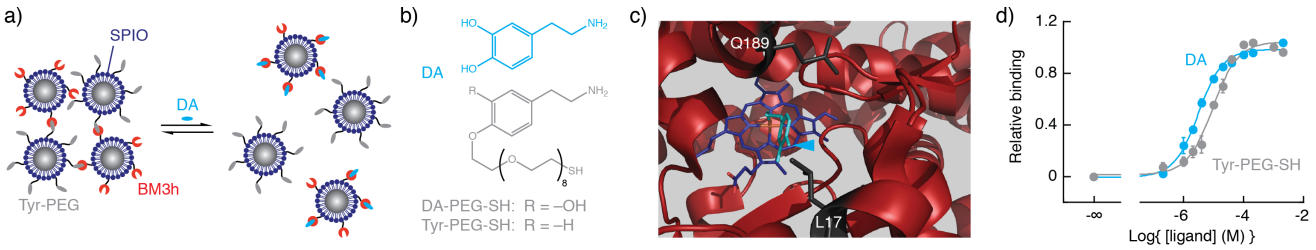

Figure 1. Design of dopamine-responsive nanosensors. (a) Architecture of DaReNas based on dopamine (DA)-dependent reversible aggregation of SPIOs. (b) Comparison of structures of dopamine and sulfhydryl-modified tethered dopamine analogs. (c) Structure of BM3h-9D7, with dopamine (cyan) bound near the protein's heme group (dark blue). White labels indicate residues whose mutation facilitates modification of the ligand at the 4-hydroxy position (arrowhead). (d) Titration curves showing similar K_d values for dopamine and Tyr-PEG-SH binding to the BM3h derivative 9D7*. Error bars depict s.e.m. of three measurements.

breaking up the aggregates and resulting in r_2 values more like unfunctionalized SPIOs.

To synthesize DaReNas, we chose to incorporate BM3h dopamine-binding proteins as actuating domains. The most effective variant, BM3h-9D7 (9D7), exhibits a reported dissociation constant (K_d) of 1.3 ± 0.1 μM and 28-fold selectivity against norepinephrine.[6] We introduced a thiol for bioconjugation of this variant to SPIOs, forming 9D7-S450C. We also sought a dopamine analog that could be tethered to thiol-reactive SPIOs while retaining affinity for 9D7. Guided by structural data,[6] we initially synthesized 4-*O*-(26-mercapto-3,6,9,12,15,18,21,24-octaoxahexacosyl)-dopamine (DA-PEG-SH, Figure 1b and Scheme S1).

Ligand binding to 9D7-S450C was examined by optical titration, exploiting absorbance changes arising from BM3h heme-analyte interactions.[5,13] Measured K_d values for binding of dopamine and DA-PEG-SH to 9D7-S450C are 1.3 ± 0.1 μM and 108 ± 1 μM, respectively, indicating that addition of the PEG-SH tether to dopamine substantially interferes with binding. To form a ligand-protein pair with improved affinity, we introduced mutations L17A and Q189T to create 9D7*, which we predicted from the 9D7-dopamine crystal structure would exhibit improved tolerance for PEGylated ligands (Figure 1c and Table S1).

We also examined the effect of eliminating the 3-hydroxy group from DA-PEG-SH, resulting in the compound *O*-(26-mercapto-3,6,9,12,15,18,21,24-octaoxahexacosyl)-tyramine (Tyr-PEG-SH, Figure 1b and Scheme S2). Tyramine has previously been shown to display minimal binding to dopamine receptors,[14] suggesting lesser potential for physiological side-effects. Optical titration of dopamine and Tyr-PEG-SH onto 9D7* yields K_d values of 2.1 ± 0.6 μM and 7.8 ± 2.6 μM, respectively (Figure 1d), indicating that the desired improvements were achieved while also preserving dopamine specificity (Figure S1).

Tyr-PEG-SH and 9D7* were subsequently conjugated to maleimide-terminated photocrosslinked lipid-coated SPIOs.[15] Following thiol-maleimide conjugation, the concentration of conjugated Tyr-PEG ligands per mM SPIO Fe was ~5 μM. Meanwhile, a standard protein assay indicated that the concentration of 9D7* domains per mM Fe was ~3 μM.

A functional DaReNa was formed by 1:1 mixing of 9D7*- and Tyr-PEG-functionalized SPIOs. The resulting nanosensor was characterized by MRI and dynamic light scattering (DLS). The average DaReNa relaxivity is 208 ± 2 (mM Fe)$^{-1}$s^{-1}, whereas r_2 values of 9D7*-SPIO and Tyr-PEG-SPIO conjugates alone range from 130-140 (mM Fe)$^{-1}$s^{-1} (Figure 2a). These values correspond to greater darkening of MRI signal by DaReNa compared with individual SPIO species, and are also consistent with DLS results demonstrating that DaReNa components cluster when mixed (Figure 2b). The mean hydrodynamic diameter (D_h) of DaReNa is 138 ± 4 nm, while D_h values of 52 ± 2 nm and 32 ± 1 nm are observed for 9D7*-SPIOs and Tyr-PEG-SPIOs alone. The observed relationship between particle size and r_2 is expected in a motional averaging relaxation regime.[16]

Dopamine causes unclustering of DaReNa particles and lowers r_2 accordingly. In DLS, addition of 200 μM dopamine to the DaReNa solution (100 μM Fe = ~1 nM nanoparticles) reduces the mean D_h by about 25%, to 104 ± 4 nm (Figure 2b). Corresponding changes in nanoparticle aggregation are directly observed using transmission electron microscopy of similar samples (Figure 2c). Dopamine concentrations above 40 μM also cause significant decreases in relaxivity (*t*-test $p \leq 0.02$, $n = 3$), with 500 μM dopamine producing an r_2 of 152 ± 2 (mM Fe)$^{-1}$s^{-1}, 20% lower than in the absence of dopamine (Figure 2d). Addition of equivalent amounts of serotonin or norepinephrine produce substantially smaller changes in r_2, indicating selectivity of the DaReNa response to dopamine (Figure 2e). Importantly, DaReNa responses to dopamine are achieved at a nanoparticle concentration of only 1 nM and a total 9D7* concentration of 0.2 μM, about 100 times lower than concentrations used for T_1-based dopamine sensing,[5,7] and low enough to have minimal effect on dopamine signaling in realistic applications.

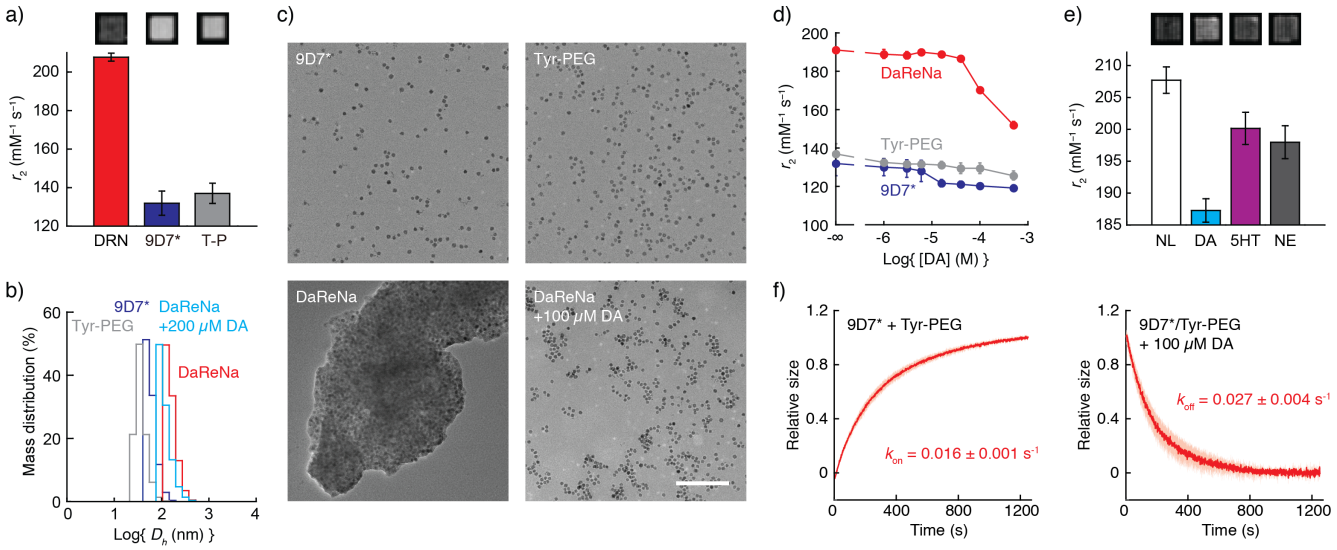

Figure 2. Response properties of DaReNa sensors. (a) T_2-weighted MRI scans (top) and relaxivity values (bars) corresponding to DaReNas (DRN), 9D7*-functionalized SPIOs (9D7*), and Tyr-PEG-functionalized SPIOs (T-P). (b) DLS size histograms of DaReNa, control nanoparticles, and DaReNa plus 200 μM dopamine (DA). (c) Transmission electron microscopy analysis of DaReNa components alone (top) and together (bottom) in absence (left) and presence (right) of 200 μM dopamine. Scale bar = 200 nm. (d) Relaxometric titration of DaReNas and control nanoparticles with dopamine. (e) MRI scans and relaxivity values showing DaReNa r_2 values without ligand (NL), or in presence of 50 μM dopamine, serotonin (5HT), or norepinephrine (NE). [SPIO Fe] = 100 μM. Error bars depict s.e.m. for three measurements. (f) BLI measurements the DaReNa mechanism kinetics. Left: Normalized time course of apparent size increases immediately following addition of Tyr-PEG-functionalized SPIOs to a 9D7*-functionalized BLI probe. Right: Unbinding of Tyr-PEG-functionalized SPIOs from the 9D7*-functionalized BLI probe after challenge with 100 μM dopamine. [SPIO Fe] = 300 μM. Shading denotes s.d. of three replicates. Response rates (k_{on} and k_{off}) reported as mean and s.e.m.

To evaluate the kinetics of the DaReNa responses, we began by examining the time course of light scattering changes after mixing 9D7* and Tyr-PEG-functionalized particles or challenging DaReNa with dopamine (Figure S2). Results obtained with a dead time of ~20 s indicate that substantial size alterations occur soon after changes in conditions, but that slow evolution of the scattering signal continues. Because light scattering tends to be dominated by large species, we also obtained more precise kinetic measurements using biolayer interferometry (BLI). 9D7* was immobilized on the surface of a BLI probe and binding and unbinding of Tyr-PEG-functionalized SPIOs were measured on a time scale of seconds. Measurements reveal an association rate of 0.016 ± 0.001 s^{-1} in the absence of dopamine and a dissociation rate of 0.027 ± 0.004 s^{-1} following challenge with 100 μM dopamine (Figure 2f). These results, which correspond to time constants of 38-63 s, are comparable to kinetic measurements from the 9D7* parent protein itself, and are thus suitable for functional imaging of responses to standard block stimuli or pharmacological challenges *in vivo*.[7,17]

As an additional precursor to *in vivo* applications, we determined that intracranial infusion of DaReNa to relevant areas of the rat brain is feasible. Targeted injection of 10 μL sensor at 1 mM SPIO iron concentration produces broad staining in the striatum, where dopamine concentrations within detection range of the sensor have previously been recorded (Figure 3).[18] T_2-weighted contrast is visible over a diameter of ~2 mm and corresponds to T_2 relaxation rate (R_2) increases by about a factor of three near the center of the injected region, revealing the ability of DaReNa to spread effectively in tissue. Noninvasive brain delivery strategies could be used in the future to further improve the distribution of sensor particles.[19]

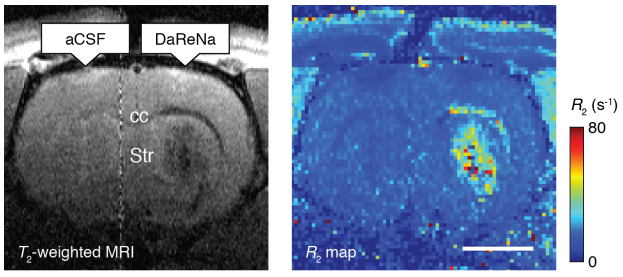

Figure 3. Targeted brain delivery of DaReNa. T_2-weighted MRI (left) and T_2 relaxation rate (R_2) maps (right) showing spreading of DaReNa in brain following unilateral infusion of 10 μL sensor ([SPIO Fe] = 1 mM). Contrast and relaxation enhancement are clearly visible near the striatal injection site (Str) and along the corpus callosum (cc). Infusion of artificial cerebrospinal fluid (aCSF) in the opposite hemisphere produces no discernable effects. Scale bar = 2 mm.

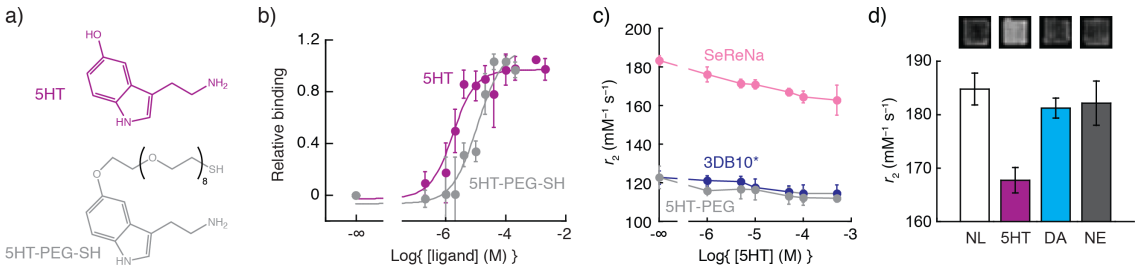

Figure 4. Design and performance of SeReNas. (a) Comparison of structures of serotonin (5HT) and 5HT-PEG-SH. (b) Titration curves showing similar binding behavior to the BM3h derivative 3DB10*. (c) Relaxivity as a function of serotonin concentration for SeReNas and SPIOs conjugated to 3DB10* or 5HT-PEG-SH alone ([SPIO Fe] = 100 μM). (d) T_2-weighted MRI (top) and r_2 values (bars) of SeReNa samples in absence of ligand (NL) and in presence of 50 μM serotonin, dopamine (DA), or norepinephrine (NE). Error bars represent s.e.m. for $n = 3$.

To demonstrate generality of neurotransmitter sensing using the DaReNa architecture, we next formulated a serotonin-responsive nanoparticle (SeReNa) probe for T_2-weighted MRI. In place of Tyr-PEG-SH, we synthesized a tethered serotonin analog, *O*-(26-mercapto-3,6,9,12,15,18,21,24-octaoxahexacosyl)-serotonin (5HT-PEG-SH, Figure 4a and Scheme S3). This molecule is similar to *O*-alkylserotonin derivatives with sharply reduced affinity for serotonin receptors,[20] but it exhibits high affinity for a previously identified serotonin-binding BM3h variant, BM3h-3DB10, which is selective against binding to dopamine and norepinephrine.[6] 3DB10 was modified for bioconjugation via the S450C mutation to produce 3DB10*. Optical titration of 3DB10* with serotonin and 5HT-PEG-SH gives K_d values of 0.95 ± 0.88 μM and 3.2 ± 5.0 μM, respectively, indicating that the protein is able to tolerate PEGylation of serotonin without substantial loss of affinity (Figure 4b).

SeReNas were generated by conjugating 3DB10* and 5HT-PEG-SH to SPIOs. Absorbance measurements indicated approximately 9 μM 5HT-PEG ligands and 3 μM 3DB10* domains per mM SPIO Fe. SeReNas display r_2 and D_h values substantially greater than those of 3DB10*- or 5HT-PEG-conjugated SPIOs (Figure S3). In contrast to DaReNas, SeReNas display less cooperative behavior when titrated with their ligand. Values of r_2 decrease almost linearly with serotonin, ranging from 183 ± 3 $(\text{mM Fe})^{-1}\text{s}^{-1}$ without ligand to 163 ± 8 $(\text{mM Fe})^{-1}\text{s}^{-1}$ in 500 μM serotonin (Figure 4c). Serotonin concentrations as low as 5 μM produce significant r_2 changes (t-test $p = 0.02$, $n = 3$), and the maximum r_2 change over the full range is 11% of the ligand-free value. These responses are selective: 50 μM serotonin produces a 9.2 % decrease in r_2, while 50 μM dopamine and norepinephrine produce changes of <1.9% (Figure 4d). As with the DaReNas, SeReNas display sensitivity at ligand binding capacities about 100-fold lower than previously used in T_1-weighted sensing approaches.

These results demonstrate that neurotransmitter sensors for T_2-weighted MRI can be formed by conjugating neurotransmitter binding proteins and cognate tethered neurotransmitters to SPIOs. DaReNas and SeReNas operate at nanoparticle concentrations of 1 nM and binding capacities of 0.2 μM, suitable for minimal perturbations to endogenous neurotransmitter concentrations ranging from micromolar in interstitium to millimolar near synapses.[21] The probes could be further refined to enhance their sensitivity, dynamic range, and kinetics. Manipulations of nanoparticle size and functionalization density, for instance, could be used to improve response times to the single-second or subsecond scale.[15,22] The combination of protein and tethered ligand engineering techniques applied here could also be used to construct MRI sensors for additional targets.

ASSOCIATED CONTENT

Supporting Information. Additional data, detailed methods, and characterization of synthetic compounds. This material is available free of charge at http://pubs.acs.org.

AUTHOR INFORMATION

Corresponding Author

jasanoff@mit.edu

Author Contributions

VH and SO contributed equally, and IGA and AB also contributed equally.

ACKNOWLEDGMENT

This work was supported by a Dana Foundation Brain and Immuno-Imaging grant, as well as NIH grants R01-DA038642, R01-DA02899, and R21-DA044748 to AJ. VH was supported by an NSERC Post-Graduate Scholarship and a Friends of the McGovern Institute Fellowship. SO was supported by a JSPS Postdoctoral Fellowship for Research Abroad and an Uehara Memorial Foundation postdoctoral fellowship. IGA was supported by fellowship from the Madrid-MIT M+Vision Consortium. RO was supported by a DFG Research Fellowship.

REFERENCES

(1) Piel, M.; Vernaleken, I.; Rosch, F. Positron emission tomography in CNS drug discovery and drug monitoring. *J Med Chem* **2014**, 57, 9232.

(2) Angelovski, G.; Toth, E. Strategies for sensing neurotransmitters with responsive MRI contrast agents. *Chem Soc Rev* **2017**, 46, 324.

(3) Kim, E. H.; Chin, G.; Rong, G.; Poskanzer, K. E.; Clark, H. A. Optical Probes for Neurobiological Sensing and Imaging. *Acc Chem Res* **2018**, 51, 1023.

(4) Jonckers, E.; Shah, D.; Hamaide, J.; Verhoye, M.; Van der Linden, A. The power of using functional fMRI on small rodents to study brain pharmacology and disease. *Front Pharmacol* **2015**, 6, 231.

(5) Shapiro, M. G.; Westmeyer, G. G.; Romero, P. A.; Szablowski, J. O.; Kuster, B.; Shah, A.; Otey, C. R.; Langer, R.; Arnold, F. H.; Jasanoff, A. Directed evolution of a magnetic resonance imaging contrast agent for noninvasive imaging of dopamine. *Nat Biotechnol* **2010**, 28, 264.

(6) Brustad, E. M.; Lelyveld, V. S.; Snow, C. D.; Crook, N.; Jung, S. T.; Martinez, F. M.; Scholl, T. J.; Jasanoff, A.; Arnold, F. H. Structure-guided directed evolution of highly selective p450-based magnetic resonance imaging sensors for dopamine and serotonin. *J Mol Biol* **2012**, 422, 245.

(7) Lee, T.; Cai, L. X.; Lelyveld, V. S.; Hai, A.; Jasanoff, A. Molecular-level functional magnetic resonance imaging of dopaminergic signaling. *Science* **2014**, 344, 533.

(8) Hai, A.; Cai, L. X.; Lee, T.; Lelyveld, V. S.; Jasanoff, A. Molecular fMRI of Serotonin Transport. *Neuron* **2016**, 92, 754.

(9) Josephson, L.; Perez, J. M.; Weissleder, R. Magnetic Nanosensors for the Detection of Oligonucleotide Sequences. *Angew Chem Int Ed Engl* **2001**, 40, 3204.

(10) Perez, J. M.; Josephson, L.; O'Loughlin, T.; Hogemann, D.; Weissleder, R. Magnetic relaxation switches capable of sensing molecular interactions. *Nat Biotechnol* **2002**, 20, 816.

(11) Perez, J. M.; Josephson, L.; Weissleder, R. Use of magnetic nanoparticles as nanosensors to probe for molecular interactions. *Chembiochem* **2004**, 5, 261.

(12) Okada, S.; Bartelle, B. B.; Li, N.; Breton-Provencher, V.; Lee, J. J.; Rodriguez, E.; Melican, J.; Sur, M.; Jasanoff, A. Calcium-dependent molecular fMRI using a magnetic nanosensor. *Nat Nanotechnol* **2018**, 13, 473.

(13) Lewis, D. F. V. *Guide to Cytochrome P450 Structure and Function*; Taylor & Francis: New York, **2001**.

(14) Vaccari, A.; Gessa, G. [^{3}H]tyramine binding: a comparison with neuronal [^{3}H]dopamine uptake and [^{3}H]mazindol binding processes. *Neurochem Res* **1989**, 14, 949.

(15) Rodriguez, E.; Lelyveld, V. S.; Atanasijevic, T.; Okada, S.; Jasanoff, A. Magnetic nanosensors optimized for rapid and reversible self-assembly. *Chem Commun* **2014**, 50, 3595.

(16) Matsumoto, Y.; Jasanoff, A. T_2 relaxation induced by clusters of superparamagnetic nanoparticles: Monte Carlo simulations. *Magn Reson Imaging* **2008**, 26, 994.

(17) Jenkins, B. G. Pharmacologic magnetic resonance imaging (phMRI): imaging drug action in the brain. *Neuroimage* **2012**, 62, 1072.

(18) Ewing, A. G.; Bigelow, J. C.; Wightman, R. M. Direct in vivo monitoring of dopamine released from two striatal compartments in the rat. *Science* **1983**, 221, 169.

(19) Ghosh, S.; Harvey, P.; Simon, J. C.; Jasanoff, A. Probing the brain with molecular fMRI. *Curr Opin Neurobiol* **2018**, 50, 201.

(20) Glennon, R. A.; Hong, S. S.; Bondarev, M.; Law, H.; Dukat, M.; Rakhi, S.; Power, P.; Fan, E.; Kinneau, D.; Kamboj, R.; Teitler, M.; Herrick-Davis, K.; Smith, C. Binding of *O*-alkyl derivatives of serotonin at human 5-HT1D beta receptors. *J Med Chem* **1996**, 39, 314.

(21) Garris, P. A.; Ciolkowski, E. L.; Pastore, P.; Wightman, R. M. Efflux of dopamine from the synaptic cleft in the nucleus accumbens of the rat brain. *J Neurosci* **1994**, 14, 6084.

(22) Shapiro, M. G.; Atanasijevic, T.; Faas, H.; Westmeyer, G. G.; Jasanoff, A. Dynamic imaging with MRI contrast agents: quantitative considerations. *Magn Reson Imaging* **2006**, 24, 449.

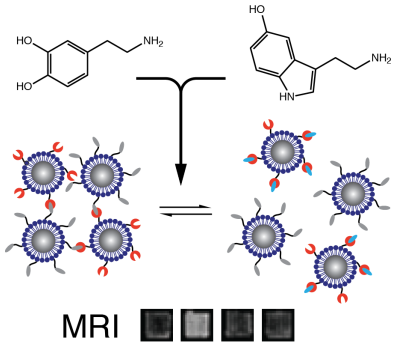
HO
HO
NH2
HO
HN
NH2
MRI